Please provide feedback

Please support the ScholarWorks@UMBC repository by emailing scholarworks-group@umbc.edu and telling us what having access to this work means to you and why it's important to you. Thank you.

Solar Wind Turbulence Around Mars: Relation Between The Energy Cascade Rate And The Proton Cyclotron Waves Activity

N. Andrés [1,2], **N. Romanelli** [3,4], **L. Z. Hadid** [5,6], **F. Sahraoui**[5], **G. DiBraccio**[3], **J. Halekas**[7]

[1]Instituto de Astronomía y Física del Espacio, CONICET-UBA, Ciudad Universitaria, 1428, Buenos Aires, Argentina
[2]Departamento de Física, UBA, Ciudad Universitaria, 1428, Buenos Aires, Argentina
[3]Solar System Exploration Division, NASA Goddard Space Flight Center, Greenbelt, MD, USA
[4]CRESST II, University of Maryland, Baltimore County, Baltimore, MD, USA.
[5]LPP, CNRS, École polytechnique, Institut Polytechnique de Paris, Sorbonne Université, F-91128 Palaiseau, France
[6]European Space Agency, ESTEC, Noordwijk, Netherlands
[7]Department of Physics and Astronomy, University of Iowa, Iowa City, Iowa, USA

Key Points:

- We estimate, for the first time, the incompressible energy cascade rate obtained in the solar wind near Mars.
- We find that the nonlinear cascade of energy is slightly amplified when proton cyclotron waves are present in the plasma.
- These statistical results show the presence of Alfvénic and non Alfvénic turbulent fluctuations in a magnetic dominant regime.

Abstract

The first estimation of the incompressible energy cascade rate at magnetohydrodynamic (MHD) scales is obtained in the plasma upstream of the Martian bow shock, using MAVEN observations and an exact relation derived for MHD turbulence. The energy cascade rate is computed for events with and without proton cyclotron wave (PCW) activity, for time intervals when MAVEN was in the solar wind with no magnetic connection to the bow shock. It is shown that the nonlinear cascade of energy at the MHD scales is slightly amplified when PCWs are present in the plasma. The analysis of the normalized cross helicity and residual energy for the turbulent fluctuations shows the presence of Alfvénic and non-Alfvénic fluctuations in a magnetic dominant regime for the majority of the cases.

Plain Language Summary

Throughout its radial expansion from the Sun, the solar wind develops a strongly turbulent regime, which can be characterized by in situ observations of proton density, velocity and magnetic field fluctuations. Turbulence serves as a reservoir of energy that cascades through the inertial range down to the smallest scales, where it is dissipated by kinetic effects. For the first time, we compute the energy cascade rate which is transferred though different scales in the inertial range. This energy rate is computed for cases with and without proton cyclotron waves activity, when MAVEN was in the solar wind. Our results show that the energy cascade rate is emphasized when waves are present in the plasma.

Corresponding author: Nahuel Andrés, `nandres@iafe.uba.ar, nandres@df.uba.ar`
https://orcid.org/0000-0002-1272-2778

1 Introduction

Turbulence is a unique phenomenon present in several space environments, like the solar corona (Hendrix & Van Hoven, 1996; Dmitruk et al., 2002), planetary environments (Sahraoui et al., 2020) or the solar wind (Bruno & Carbone, 2005; W. Matthaeus & Velli, 2011). In particular, solar wind turbulence is partially characterized by an inertial range, where energy is transferred without dissipation through different spatial and temporal scales (e.g., Frisch, 1995). Typically, in the largest magnetohydrodynamic (MHD) scales, the solar wind magnetic spectrum presents a $-5/3$ slope (Kolmogorov, 1941a,b; W. H. Matthaeus & Goldstein, 1982; Leamon et al., 1998; Chen, 2016), which is generally compatible with a constant energy cascade rate as a function of such scales (Sorriso-Valvo et al., 2007; Marino et al., 2008; Coburn et al., 2014; Coburn et al., 2015; Hadid et al., 2017). A constant energy cascade rate reflects a well accepted idea that large (MHD) scale turbulence serves as a reservoir of energy that cascades down to the smallest scales, where it can be dissipated by kinetic effects (e.g., Leamon et al., 1998; Sahraoui et al., 2009; Alexandrova et al., 2009; Andrés et al., 2014).

Assuming spatial homogeneity and full isotropy, an exact relation for fully developed incompressible MHD turbulence can be derived (Politano & Pouquet, 1998a,b). Among its potential applications (e.g., Weygand et al., 2007; W. H. Matthaeus et al., 1999; MacBride et al., 2008; Benzi et al., 1993; Grossmann et al., 1997; Andrés & Banerjee, 2019), the exact relation provides a precise computation of the amount of energy per unit time and volume (or heating rate) as a function of the velocity and magnetic correlation functions. The MHD exact relation and its connection with the nonlinear energy cascade rate has been numerically validated for both incompressible and compressible MHD turbulence (Andrés et al., 2018), and has been generalized to include sub-ion scale effects (Andrés et al., 2018, 2019; Hadid et al., 2018; Hellinger et al., 2018; Ferrand et al., 2019; Banerjee & Andrés, 2020). Estimations of the energy cascade rate in the inertial range of solar wind turbulence have been previously computed at 1 Astronomical Unit (AU) (see, Marino et al., 2008; Coburn et al., 2014; Coburn et al., 2015; Banerjee et al., 2016; Hadid et al., 2017) and more recently at ~ 0.2 AU (Bandyopadhyay et al., 2020; Chen et al., 2020). In particular, Hadid et al. (2017) have investigated in detail the role of the compressible fluctuations (Banerjee & Galtier, 2013; Andrés & Sahraoui, 2017) in modifying the energy cascade rate with respect to the prediction of the incompressible MHD model, based in situ data from the THEMIS/ARTEMIS spacecraft in the fast and slow solar wind.

The induced magnetosphere of Mars is formed as a result of the interaction between the solar wind and the planet's atmosphere, including its exosphere, ionosphere and the crustal magnetic fields (Acuña, 1998, 1999). This interaction starts upstream of the Martian bow shock, due to the lack of an intrinsic global planetary magnetic field and the presence of an extended hydrogen exosphere (e.g., Chaffin et al., 2015). The response of this atmospheric obstacle is significantly modified by time-dependent physical processes (e.g., Edberg et al., 2010; Jakosky et al., 2015b; Romanelli et al., 2018a), as a result of temporal variability of the planetary and solar wind properties over different timescales (e.g., Edberg et al., 2009; Modolo et al., 2012; Ma et al., 2014; Fang et al., 2015; Romanelli et al., 2018b, 2019). The seasonal variability of the Martian hydrogen exosphere has been identified by several spacecraft (Bhattacharyya et al., 2015; Chaffin et al., 2014; Clarke et al., 2014, 2017; Halekas et al., 2017; Halekas, 2017). In particular, the Martian exosphere is subject to several ionizing mechanisms giving rise to newborn planetary protons, allowing one to indirectly observe such seasonal dependence with plasma instruments (e.g., Yamauchi et al., 2015; Rahmati et al., 2017). For instance, higher pickup ions detection rates were observed when Mars is near perihelion (Yamauchi et al., 2015). Moreover, when available, the measurement of the resulting proton velocity distribution function at these altitudes is composed of a core of solar wind particles and a non thermal proton population due to the presence of newborn planetary ions (seen in the solar wind reference frame). Such particle velocity distribution function is highly unstable and can give rise to several ultra-low frequency plasma waves (C. S. Wu & Davidson, 1972; C. Wu & Hartle, 1974; Brinca, 1991; Gary, 1991; Mazelle & Neubauer, 1993; Cowee et al., 2012).

In addition to their capability to excite different plasma waves, the relative velocity between the newborn planetary proton reference frame (very close to the planetary and spacecraft rest

frames) and the solar wind is also responsible for a Doppler shift that defines the observed wave frequency near the local proton cyclotron frequency in the spacecraft reference frame (e.g., Russell et al., 1990; Brain, 2002; Mazelle et al., 2004; Romanelli et al., 2013, 2016; Ruhunusiri et al., 2015, 2016; Liu et al., 2020). Variability in the proton cyclotron waves (PCWs) occurrence rate has been observed based on Mars Global Surveyor magnetic field data (Romanelli et al., 2013; Bertucci et al., 2013) and more recently with MAVEN Magnetometer (MAG) observations (Romanelli et al., 2016; Jakosky et al., 2015a; Connerney et al., 2015). In particular, Romanelli et al. (2016) have analyzed MAG observations between October 2014 and March 2016. The authors reported that the PCWs occurrence rate upstream of the Martian bow shock varies with time and takes higher values near the Martian perihelion. Such long term trend was associated with higher hydrogen exospheric densities around that orbital position (derived from numerical simulations) and was also in agreement with the long term trend observed in the irradiances in the 121-122 nm range by MAVEN extreme ultra-violet monitor (EUVM) measurements (Eparvier et al., 2015), which provide a proxy to study the temporal variability of the photoionization frequency of the neutral H exosphere.

Ruhunusiri et al. (2017) have characterized magnetic energy spectra in the Mars plasma environment using the MAVEN MAG observations, in the frequency range 0.005 Hz to 16 Hz. By computing the spectral indices for the magnetic energy, the authors showed a wide range of values in the upstream solar wind and the magnetosheath plasma. Also, they observed a seasonal variability of the spectral indices, indicative of a clear connection with the seasonal variability of the PCWs. Nevertheless, to the best of our knowledge, no estimation of the energy cascade rate has been reported yet in the Martian plasma environment. In the present Letter, we aim to extend the current state of knowledge of the solar wind turbulence upstream the Martian shock by computing for the first time the energy transfer rate using an exact relation for fully development turbulence. Using both magnetic field and plasma moments observations at ~ 1.8 AU, we investigate how turbulence is affected not only by the heliocentric distance, but also for the presence of PCWs.

2 Incompressible MHD Turbulence

The three-dimensional (3D) incompressible MHD equations can be written as,

$$\frac{\partial \mathbf{u}}{\partial t} = -\mathbf{u} \cdot \boldsymbol{\nabla}\mathbf{u} + \mathbf{u}_{\mathrm{A}} \cdot \boldsymbol{\nabla}\mathbf{u}_{\mathrm{A}} - \frac{1}{\rho_0}\boldsymbol{\nabla}(P + P_M) + \mathbf{f}_k + \mathbf{d}_k, \tag{1}$$

$$\frac{\partial \mathbf{u}_{\mathrm{A}}}{\partial t} = -\mathbf{u} \cdot \boldsymbol{\nabla}\mathbf{u}_{\mathrm{A}} + \mathbf{u}_{\mathrm{A}} \cdot \boldsymbol{\nabla}\mathbf{u} + \mathbf{f}_m + \mathbf{d}_m, \tag{2}$$

$$\boldsymbol{\nabla} \cdot \mathbf{u} = 0, \tag{3}$$

$$\boldsymbol{\nabla} \cdot \mathbf{u}_{\mathrm{A}} = 0 \tag{4}$$

where we have defined the incompressible Alfvén velocity $\mathbf{u}_{\mathrm{A}} \equiv \mathbf{B}/\sqrt{4\pi\rho_0}$ (where ρ_0 the mean mass density) and $P_M \equiv \rho_0 u_{\mathrm{A}}^2/2$ is the magnetic pressure. Then, both field variables, $\mathbf{u}$ and $\mathbf{u}_{\mathrm{A}}$, are expressed in speed units. Finally, $\mathbf{f}_{k,m}$ are respectively a mechanical and the curl of the electromotive large-scale forcings, and $\mathbf{d}_{k,m}$ are respectively the small-scale kinetic and magnetic dissipation terms (Andrés, Mininni, et al., 2016; Banerjee & Kritsuk, 2018).

Using Eq. (1)-(4) and following the usual assumptions for fully developed homogeneous turbulence (i.e., infinite kinetic and magnetic Reynolds numbers and a steady state with a balance between forcing and dissipation (see, e.g. Andrés & Sahraoui, 2017), an exact relation for incompressible MHD turbulence can be obtained as (Politano & Pouquet, 1998a,b),

$$-4\varepsilon = \rho_0 \boldsymbol{\nabla}_\ell \cdot \langle (\delta\mathbf{u} \cdot \delta\mathbf{u} + \delta\mathbf{u}_{\mathrm{A}} \cdot \delta\mathbf{u}_{\mathrm{A}})\delta\mathbf{u} - (\delta\mathbf{u} \cdot \delta\mathbf{u}_{\mathrm{A}} + \delta\mathbf{u}_{\mathrm{A}} \cdot \delta\mathbf{u})\delta\mathbf{u}_{\mathrm{A}}\rangle, \tag{5}$$

where ε is the total energy cascade rate per unit volume. Fields are evaluated at position $\mathbf{x}$ or $\mathbf{x}' = \mathbf{x} + \boldsymbol{\ell}$; in the latter case a prime is added to the field. The angular bracket $\langle\cdot\rangle$ denotes an ensemble average (Batchelor, 1953), which is taken here as time average assuming ergodicity. Finally, we have introduced the usual increments definition, i.e., $\delta\alpha \equiv \alpha' - \alpha$. Here is we are interested in estimating ε from Eq. (5), which is fully defined by velocity and magnetic field increments (or fluctuations) that we can estimate from MAVEN observations.

3 Analysis and Results

3.1 MAVEN observations

The MAVEN Magnetometer (MAG) provides vector magnetic field measurements with a 32 Hz maximum sampling frequency and absolute vector accuracy of 0.05% (Connerney et al., 2015). MAVEN's Solar Wind Ion Analyzer (SWIA) is an energy and angular ion spectrometer covering an energy range between 25 eV/q and 25 keV/q with a field of view of $360° \times 90°$ (Halekas et al., 2015). In this study, we have analyzed the MAVEN MAG and SWIA data sets as follows. Magnetic field observations with 32 Hz cadence are analyzed to discriminate events in the pristine solar wind with PCWs and without wave activity. To estimate the energy cascade rate at MHD scales (i.e., frequencies below ~ 0.1 Hz) we averaged the magnetic field data over 4 s to match SWIA onboard moments cadence (Halekas et al., 2015).

As discussed in the Introduction, Romanelli et al. (2016) have found that the PCWs occurrence rate increases (up to $\sim 50\%$) when Mars is close to the perihelion (1.38 AU) on December 12 2014 and remains relatively low and constant ($\sim 25\%$) after reaching the Martian Northern Spring Equinox-Southern Autumn Equinox (NSE-SAE). Also, the authors concluded that the increment in the PCWs occurrence rate cannot be the result of biases associated with MAVEN's spatial coverage of the upstream region or of the differences in the spatial distribution of the crustal magnetic fields. Therefore, to investigate how PCWs activity may affect the nonlinear transfer of energy, we consider two data sets. Set A contains observations from December 1 2014 until January 31 2015; and set B from January 1, 2015 until February 29, 2016. Set A includes MAVEN observations around perihelion and a local maximum of PCWs activity, while set B includes the Martian Northern Summer Solstice-Southern Winter Solstice (NSS-SWS) that took place on January 3 2016 (and corresponds to a local minimum of waves activity).

3.2 Selection criteria

For sets A and B (~ 330 orbits per set), during time periods when MAVEN was traveling in the solar wind with no connection to the shock (Gruesbeck et al., 2018), we looked for intervals in which the number density fluctuation level was lower than 20% (to be as close as possible to the incompressibilty condition). Moreover, in order to have reliable estimate of the energy cascade rate ε (both its sign and its absolute value (Halekas et al., 2017)) we only consider the events in which the θ_{uB} (the angle between the magnetic and velocity field) was relatively stationary (Andrés et al., 2019). The long time intervals that fulfil these criteria were divided into a series of sample events with a duration of 30 minutes. This duration ensures having at least one correlation time of the turbulent fluctuations (Hadid et al., 2017; Marquette et al., 2018). Finally, for set A (set B) we considered only cases when PCWs activity was present (absent). By doing this, we can assess the effects that the PCWs may have on the solar wind turbulence. This selection eventually resulted in 184 and 208 events for sets A and B, respectively.

Figure 1 shows two examples of the typical events analyzed in the present Letter (panels (a)-(h) show an example from set A, and panels (i)-(p) from set B). Figure 1 (a)-(f) show the time series for the proton and Alfvén velocity field components in Mars-centered Solar Orbital (MSO) coordinate system (where the **x**-axis points from Mars to the Sun, **z**-axis is perpendicular to Mars' orbital plane and is positive toward the ecliptic north; the **y**-axis completes the right-handed system). Figure 1 (g)-(h) show the angle between the magnetic and velocity field θ_{uB} and the density fluctuation level (i.e., $\Delta n / \langle n \rangle$), respectively. Both examples show approximately the same level of density fluctuations and the same θ_{uB} angle. Finally, the Supporting Information shows that both sets A and B have similar distributions for the density, velocity and magnetic fluctuation values.

3.3 PSD of the magnetic field fluctuations

To determine if a given time interval presents PCWs activity or not, we used a criterion similar to the one in Romanelli et al. (2016). An event is considered to present PCWs activity when the magnetic energy power spectral density (PSD) displays an increase in a frequency interval centered

around the local proton cyclotron frequency f_{ci} when compared to two contiguous windows of width $0.2\ f_{ci}$. More precisely,

$$max\{\text{PSD}[B(f)]|_{0.8f_{ci}}^{1.2f_{ci}}\} > max\{\text{PSD}[B(f)]|_{1.2f_{ci}}^{1.4f_{ci}}\}, max\{\text{PSD}[B(f)]|_{0.6f_{ci}}^{0.8f_{ci}}\} \qquad (6)$$

where *max* corresponds to the maximum value in the PSD in the corresponding window.

Figure 2 (a) and (b) show the PSD for all the events in sets A and B, respectively. For reference, we plot a straight line with Kolmogorov-like slope (i.e., -5/3) in both cases. As we expected, all events near the Martian perihelion (i.e., set A) show a clear peak in their PSD near the proton cyclotron frequency f_{ci}. Moreover, all the cases analyzed in the present Letter show a Kolmogorov-like slope in the MHD scales (see, Ruhunusiri et al., 2017). The inset in Figure 2 (a) and (b) show the MAVEN location (where $\text{R}_{\text{MSO}} = \sqrt{y_{\text{MSO}}^2 + z_{\text{MSO}}^2}$) for each event for sets A and B, respectively. Finally, the gray dashed line corresponds to best fit of the bow shock extract from Gruesbeck et al. (2018).

3.4 Energy cascade rates

To compute the right hand side of Eq. (5), we constructed temporal correlation functions of the different turbulent fields at different time lags τ in the interval [4,1800] s, which allows covering the MHD inertial range (Ruhunusiri et al., 2017; Hadid et al., 2017). More precisely, assuming the Taylor hypothesis (i.e., $\tau \equiv \ell/V$, where V is the mean plasma flow speed), Eq. (5) can be expressed as a function of time lags τ. Therefore, for each event in both sets, we compute $\varepsilon(\tau)$.

Figure 3 (a) and (b) show the absolute value of the energy cascade rate as a function of the time lag (τ) for both sets. Figure 3 (c) shows the histogram for the (log) mean values $\log\langle|\varepsilon|\rangle_{\text{MHD}}$ in the MHD scales ($\tau = 5 \times 10^2 - 1.5 \times 10^3$ s). It is worth emphasizing that if ε is changing significantly in amplitude and/or sign, then the resulting mean values would not be reliable (see, e.g., Hadid et al., 2018; Andrés et al., 2019). Therefore, as we mentioned before, we kept only the intervals for which the cascade rate shows a constant (negative or positive) sign for all the time lags in the MHD range. By doing so, the mean value of ε for each event is robust and so is its absolute value (Coburn et al., 2015; Hadid et al., 2018). The only limitation of analyzing the non-signed ε is related to the direct vs. inverse nature of the energy cascade rate. This is because the convergence of the sign of ε is more stringent than its absolute value (see, Coburn et al., 2015; Hadid et al., 2018), thus demanding a much larger statistical sample than the one considered in the present work. For both data set A and B, the cascade rate values are lower than the averaged value observed at 1 AU, $\varepsilon \sim 10^{-16} - 10^{-17}$ J m^{-3} s^{-1} (Hadid et al., 2018). Also, it is worth mentioning that the energy cascade rate slightly increases when PCWs are present in the solar wind, based on our statistical analysis.

3.5 Alfvénic fluctuations

The cross helicity $H_c = \langle\mathbf{u} \cdot \mathbf{u}_\text{A}\rangle$ and the total energy $E_T \equiv (\langle|\mathbf{u}|^2\rangle + \langle|\mathbf{u}_\text{A}|^2\rangle)/2$ (where $\mathbf{u}$ and $\mathbf{u}_\text{A}$ are the proton and Alfén velocities fluctuations) are the two rugged invariant of the ideal incompressible MHD model (see Eqs. 1-4). The dimensionless measure of the normalized cross-helicity corresponds to $\sigma_c \equiv H_C/E_T$, with $-1 \leq \sigma_c \leq 1$. Usually, fluctuations with $|\sigma_c| \sim 1$ are described as being Alfvénic. Another related measurement to quantify the relative energy present in the kinetic and magnetic fluctuations is the normalized residual energy $\sigma_r \equiv (\langle|\mathbf{u}|^2\rangle - \langle|\mathbf{u}_\text{A}|^2\rangle)/E_T$. This parameter also range between -1 and 1.

Figure 4 shows the scatter plot of σ_r as a function of σ_c, for both sets A and B, respectively. The colorbar corresponds to the mean value of the energy cascade rate in the MHD scales $\langle|\varepsilon|\rangle_{\text{MHD}}$. The statistical results show a wide variety of possible values of σ_r and σ_c, independently of the presence of PCWs. However, for set B, the events gather around $|\sigma_c| \sim 0.75$ and $\sigma_r \sim -0.4$.

4 Discussions and Conclusions

In the present work, we analyzed two data sets by considering separately the cases with (set A) and without PCWs (set B). In agreement with previous studies, our findings are consistent with the seasonal variability of PCWs (Romanelli et al., 2013; Bertucci et al., 2013; Romanelli et al., 2016). We confirmed that such variability is not the result of biases associated with the spatial coverage of MAVEN or with changes in the background velocity or magnetic fields.

Our statistical results show slopes compatible with a Kolmogorov scaling in the largest MHD scales in both sets. Ruhunusiri et al. (2017) determined spectra of magnetic field fluctuations in order to characterize turbulence in the Mars plasma environment. Using 512 s sliding windows, the authors found that magnetic spectrum slopes present different values. In particular, they found that the slope is typically ~ -1.2 at the solar wind (in the MHD scales), which differs from the Kolmogorov spectrum. This discrepancy between the computed slopes could be due to several factors: i) we are including only the cases where the cascade rate and the angle θ_{uB} are approximately constant; ii) the sliding window size used in Ruhunusiri et al. (2017) may not include enough correlation times to yield reliable PSD slopes; and iii) we are separating between PCWs and no waves events, while Ruhunusiri et al. (2017) included all the available data. It is worth mentioning that Gurnett et al. (2010) showed that the magnetic field fluctuations have a Kolmogorov scaling using magnetic field values derived from electron cyclotron echoes from Mars Express observations. Also, the $f^{-5/3}$ spectrum for the magnetic energy is theoretically compatible with our constant energy cascade rate assumption (Andrés, Mininni, et al., 2016; Andrés, Galtier, & Sahraoui, 2016).

We found that the energy cascade rate at Mars (~ 1.8 AU) decreases comparing with previous results at 1 AU and smaller distance from the Sun (see, W. Matthaeus & Velli, 2011; Bruno & Carbone, 2005; Hadid et al., 2017; Bandyopadhyay et al., 2020). In particular, the statistical results for the data set B (no presence of PCWs activity) show a decrease of $|\varepsilon|$ of at least 1 order of magnitude with respect to the value at 1 AU (i.e., $10^{-16} - 10^{-17}$ J m^{-3} s^{-1}) (Hadid et al., 2018). However, for the data set A, we observe a slight increase in the transfer of energy when waves are present in the plasma. Our results suggest that PCWs at the sub ion scales may affect the turbulence properties at the MHD scales. In other words, while Eq. (5) is valid *only* in the MHD inertial range, our results suggest that the instabilities and consequent nonlinear waves at frequencies $\sim f_{ci}$ may affect the largest MHD scales (Osman et al., 2013; Hadid et al., 2018). However, although several theoretical papers have shown that newborn planetary ions are capable of providing the free energy for the presence of PCWs (e.g., Brinca, 1991), the PCWs observed upstream from the Martian bow shock are nonlinear and likely not saturated (Cowee et al., 2012). While a increase in $|\varepsilon|$ in correlation with PCWs activity has not been observed before, an analysis of the local velocity distribution functions is still needed to better characterize the growing stage of the observed PCWs and its connection with the reported results.

While both sets show similar values in the parameter space of number density, velocity and Alfvén velocity fields values, our results show a wide variability in the possible values of σ_c and σ_r. In particular, the events in set B correspond to Alfvénic and magnetic dominant fluctuations ($|\sigma_c| \sim 0.75$ and $\sigma_r \sim -0.4$). Interestingly, these events correspond to the higher values of the cascade rate in the set B. Moreover, for both sets the events have mainly negative σ_r values with a majority gathering around $\sigma_r \sim -0.25$ and $\sigma_r \sim -0.4$, respectively. This majority of events in the magnetic dominant regime is compatible with previous results between 1 and 8 AU (Roberts et al., 1990; Bruno et al., 2007; Halekas et al., 2017). In particular, Halekas et al. (2017) have investigated the spatial distributions of σ_r and σ_c using 30 minutes time intervals with a 45 s cadence. Separating observations into four subsets based on the B_y sign and the time range (near perihelion or aphelion), the authors found that the temporal decrease in σ_c appears to be equally present in all upstream regions sampled by MAVEN. Our results using 4 s or 45 s (not shown here) cadence exhibit a similar statistical trend. Therefore, the PCWs activity is not affecting significantly the mean value of the statistical distributions of σ_r and σ_c. Slight differences with Halekas et al. (2017) are probably due to the considered selection criteria.

Finally, in this study we have not computed the compressible component of the energy cascade rate (Banerjee & Galtier, 2013; Andrés & Sahraoui, 2017). In particular, we expect to obtain an

strong increases in the nonlinear cascade rate of energy in the Martian magnetosheath, where compressibility plays a major role, like in the Earth's magnetosheath (Hadid et al., 2018; Andrés et al., 2019). Furthermore, a possible seasonal variability of the incompressible and/or compressible energy cascade rate may be present in the Martian environment. These studies will be part of future works.

Acknowledgments

References

Acuña, M. H. (1998, March). Magnetic field and plasma observations at mars: Initial results of the mars global surveyor mission. *Science*, *279*(5357), 1676–1680.

Acuña, M. H. (1999, April). Global distribution of crustal magnetization discovered by the mars global surveyor MAG/ER experiment. *Science*, *284*(5415), 790-793.

Alexandrova, O., Saur, J., Lacombe, C., Mangeney, A., Mitchell, J., Schwartz, S. J., & Robert, P. (2009, Oct). Universality of solar-wind turbulent spectrum from mhd to electron scales. *Phys. Rev. Lett.*, *103*, 165003. Retrieved from https://link.aps.org/doi/10.1103/PhysRevLett.103.165003 doi: 10.1103/PhysRevLett.103.165003

Andrés, N., & Banerjee, S. (2019, Feb). Statistics of incompressible hydrodynamic turbulence: An alternative approach. *Phys. Rev. Fluids*, *4*, 024603. Retrieved from https://link.aps.org/doi/10.1103/PhysRevFluids.4.024603 doi: 10.1103/PhysRevFluids.4.024603

Andrés, N., Galtier, S., & Sahraoui, F. (2016). Exact scaling laws for helical three-dimensional two-fluid turbulent plasmas. *Physical Review E*, *94*(6), 063206.

Andrés, N., Galtier, S., & Sahraoui, F. (2018). Exact law for homogeneous compressible hall magnetohydrodynamics turbulence. *Physical Review E*, *97*(1), 013204.

Andrés, N., Gonzalez, C., Martin, L., Dmitruk, P., & Gómez, D. (2014). Two-fluid turbulence including electron inertia. *Physics of Plasmas*, *21*(12), 122305.

Andrés, N., Mininni, P. D., Dmitruk, P., & Gomez, D. O. (2016). von kármán–howarth equation for three-dimensional two-fluid plasmas. *Physical Review E*, *93*(6), 063202.

Andrés, N., & Sahraoui, F. (2017). Alternative derivation of exact law for compressible and isothermal magnetohydrodynamics turbulence. *Physical Review E*, *96*(5), 053205.

Andrés, N., Sahraoui, F., Galtier, S., Hadid, L. Z., Ferrand, R., & Huang, S. Y. (2019). Energy cascade rate measured in a collisionless space plasma with mms data and compressible hall magnetohydrodynamic turbulence theory. *Physical Review Letters*, *123*(24), 245101.

Andrés, N., Sahraoui, F., Galtier, S., Hadid, L. Z., Dmitruk, P., & Mininni, P. D. (2018). Energy cascade rate in isothermal compressible magnetohydrodynamic turbulence. *Journal of Plasma Physics*, *84*(4), 905840404. doi: 10.1017/S0022377818000788

Bandyopadhyay, R., Goldstein, M., Maruca, B., Matthaeus, W., Parashar, T., Ruffolo, D., . . . others (2020). Enhanced energy transfer rate in solar wind turbulence observed near the sun from parker solar probe. *The Astrophysical Journal Supplement Series*, *246*(2), 48.

Banerjee, S., & Andrés, N. (2020, Apr). Scale-to-scale energy transfer rate in compressible two-fluid plasma turbulence. *Phys. Rev. E*, *101*, 043212. Retrieved from https://link.aps.org/doi/10.1103/PhysRevE.101.043212 doi: 10.1103/PhysRevE.101.043212

Banerjee, S., & Galtier, S. (2013). Exact relation with two-point correlation functions and phenomenological approach for compressible magnetohydrodynamic turbulence. *Physical Review E*, *87*(1), 013019.

Banerjee, S., Hadid, L. Z., Sahraoui, F., & Galtier, S. (2016). Scaling of compressible magnetohydrodynamic turbulence in the fast solar wind. *The Astrophysical Journal Letters*, *829*(2), L27.

Banerjee, S., & Kritsuk, A. G. (2018, Feb). Energy transfer in compressible magnetohydrody-

namic turbulence for isothermal self-gravitating fluids. *Phys. Rev. E*, *97*, 023107. Retrieved from https://link.aps.org/doi/10.1103/PhysRevE.97.023107 doi: 10.1103/PhysRevE.97 .023107

Batchelor, G. K. (1953). *The theory of homogeneus turbulence.* Cambridge Univ. Press.

Benzi, R., Ciliberto, S., Tripiccione, R., Baudet, C., Massaioli, F., & Succi, S. (1993). *Phys. Rev. E*, *48*, R29.

Bertucci, C., Romanelli, N., Chaufray, J. Y., Gomez, D., Mazelle, C., Delva, M., . . . Brain, D. A. (2013). Temporal variability of waves at the proton cyclotron frequency upstream from mars: Implications for mars distant hydrogen exosphere. *Geophysical Research Letters*, *40*(15), 3809-3813. Retrieved from https://agupubs.onlinelibrary.wiley.com/doi/abs/10.1002/grl.50709 doi: 10.1002/grl.50709

Bhattacharyya, D., Clarke, J. T., Bertaux, J.-L., Chaufray, J.-Y., & Mayyasi, M. (2015, October). A strong seasonal dependence in the martian hydrogen exosphere. *Geophysical Research Letters*, *42*(20), 8678–8685. Retrieved from https://doi.org/10.1002/2015gl065804 doi: 10 .1002/2015gl065804

Brain, D. A. (2002). Observations of low-frequency electromagnetic plasma waves upstream from the martian shock. *Journal of Geophysical Research*, *107*(A6). Retrieved from https://doi .org/10.1029/2000ja000416 doi: 10.1029/2000ja000416

Brinca, A. (1991). Cometary linear instabilities: From profusion to perspective. *Cometary plasma processes*, *61*, 211–221.

Bruno, R., & Carbone, V. (2005). The solar wind as a turbulence laboratory. *Living Reviews in Solar Physics*, *2*(1), 4.

Bruno, R., d'Amicis, R., Bavassano, B., Carbone, V., & Sorriso-Valvo, L. (2007). Magnetically dominated structures as an important component of the solar wind turbulence.

Chaffin, M. S., Chaufray, J. Y., Deighan, J., Schneider, N. M., McClintock, W. E., Stewart, A. I. F., . . . Jakosky, B. M. (2015, nov). Three-dimensional structure in the mars h corona revealed by iuvs on maven. *Geophysical Research Letters*, *42*(21), 9001-9008.

Chaffin, M. S., Chaufray, J.-Y., Stewart, I., Montmessin, F., Schneider, N. M., & Bertaux, J.-L. (2014, January). Unexpected variability of martian hydrogen escape. *Geophysical Research Letters*, *41*(2), 314–320. Retrieved from https://doi.org/10.1002/2013gl058578 doi: 10.1002/2013gl058578

Chen, C. H. K. (2016). Recent progress in astrophysical plasma turbulence from solar wind observations. *Journal of Plasma Physics*, *82*(6), 535820602. doi: 10.1017/S0022377816001124

Chen, C. H. K., Bale, S. D., Bonnell, J., Borovikov, D., Bowen, T., Burgess, D., . . . others (2020). The evolution and role of solar wind turbulence in the inner heliosphere. *The Astrophysical Journal Supplement Series*, *246*(2), 53.

Clarke, J. T., Bertaux, J.-L., Chaufray, J.-Y., Gladstone, G. R., Quemerais, E., Wilson, J. K., & Bhattacharyya, D. (2014, November). A rapid decrease of the hydrogen corona of mars. *Geophysical Research Letters*, *41*(22), 8013–8020. Retrieved from https://doi.org/10.1002/2014gl061803 doi: 10.1002/2014gl061803

Clarke, J. T., Mayyasi, M., Bhattacharyya, D., Schneider, N. M., McClintock, W. E., Deighan, J. I., . . . Jakosky, B. M. (2017, February). Variability of d and h in the martian upper atmosphere observed with the MAVEN IUVS echelle channel. *Journal of Geophysical Research: Space Physics*, *122*(2), 2336–2344. Retrieved from https://doi.org/10.1002/2016ja023479 doi: 10.1002/2016ja023479

Coburn, J. T., Forman, M. A., Smith, C. W., Vasquez, B. J., & Stawarz, J. E. (2015). Third-moment descriptions of the interplanetary turbulent cascade, intermittency and back transfer. *Philosophical Transactions of the Royal Society A: Mathematical, Physical and Engineering Sciences*, *373*(2041), 20140150. doi: 10.1098/rsta.2014.0150

Coburn, J. T., Smith, C. W., Vasquez, B. J., Forman, M. A., & Stawarz, J. E. (2014, May). Variable Cascade Dynamics and Intermittency in the Solar Wind at 1 AU. *ApJ*, *786*(1), 52. doi: 10 .1088/0004-637X/786/1/52

Connerney, J. E. P., Espley, J., Lawton, P., Murphy, S., Odom, J., Oliversen, R., & Sheppard, D. (2015, Dec 01). The maven magnetic field investigation. *Space Science Reviews*, *195*(1),

257–291.

Cowee, M. M., Gary, S. P., & Wei, H. Y. (2012, April). Pickup ions and ion cyclotron wave amplitudes upstream of mars: First results from the 1d hybrid simulation. *Geophysical Research Letters*, *39*(8), n/a–n/a. Retrieved from https://doi.org/10.1029/2012gl051313 doi: 10.1029/2012gl051313

Dmitruk, P., Matthaeus, W. H., Milano, L., Oughton, S., Zank, G. P., & Mullan, D. (2002). Coronal heating distribution due to low-frequency, wave-driven turbulence. *The Astrophysical Journal*, *575*(1), 571.

Edberg, N. J. T., Brain, D. A., Lester, M., Cowley, S. W. H., Modolo, R., Fränz, M., & Barabash, S. (2009, September). Plasma boundary variability at mars as observed by mars global surveyor and mars express. *Annales Geophysicae*, *27*(9), 3537–3550. Retrieved from https://doi.org/10.5194/angeo-27-3537-2009 doi: 10.5194/angeo-27-3537-2009

Edberg, N. J. T., Nilsson, H., Williams, A. O., Lester, M., Milan, S. E., Cowley, S. W. H., ... Futaana, Y. (2010, February). Pumping out the atmosphere of mars through solar wind pressure pulses. *Geophysical Research Letters*, *37*(3), n/a–n/a. Retrieved from https://doi.org/10.1029/2009gl041814 doi: 10.1029/2009gl041814

Eparvier, F., Chamberlin, P., Woods, T., & Thiemann, E. (2015). The solar extreme ultraviolet monitor for maven. *Space Science Reviews*, *195*(1-4), 293–301.

Fang, X., Ma, Y., Brain, D., Dong, Y., & Lillis, R. (2015). Control of mars global atmospheric loss by the continuous rotation of the crustal magnetic field: A time-dependent mhd study. *Journal of Geophysical Research: Space Physics*, *120*(12), 10–926.

Ferrand, R., Galtier, S., Sahraoui, F., Meyrand, R., Andrés, N., & Banerjee, S. (2019, May). On exact laws in incompressible Hall magnetohydrodynamic turbulence. *arXiv e-prints*.

Frisch, U. (1995). *Turbulence: The legacy of a. n. kolmogorov.* Cambridge University Press.

Gary, S. P. (1991). Electromagnetic ion/ion instabilities and their consequences in space plasmas: A review. *Space Science Reviews*, *56*(3-4), 373–415.

Grossmann, S., Lohse, D., & Reeh, A. (1997). *Phys. Rev. E*, *56*(5), 5473-.

Gruesbeck, J. R., Espley, J. R., Connerney, J. E. P., DiBraccio, G. A., Soobiah, Y. I., Brain, D., ... Mitchell, D. L. (2018). The three-dimensional bow shock of mars as observed by maven. *Journal of Geophysical Research: Space Physics*, *123*(6), 4542-4555. Retrieved from https://agupubs.onlinelibrary.wiley.com/doi/abs/10.1029/2018JA025366 doi: 10.1029/2018JA025366

Gurnett, D., Morgan, D., Duru, F., Akalin, F., Winningham, J., Frahm, R., ... Barabash, S. (2010). Large density fluctuations in the martian ionosphere as observed by the mars express radar sounder. *Icarus*, *206*(1), 83–94.

Hadid, L., Sahraoui, F., & Galtier, S. (2017). Energy cascade rate in compressible fast and slow solar wind turbulence. *The Astrophysical Journal*, *838*(1), 9.

Hadid, L., Sahraoui, F., Galtier, S., & Huang, S. (2018). Compressible magnetohydrodynamic turbulence in the earth's magnetosheath: estimation of the energy cascade rate using in situ spacecraft data. *Phys. Rev. Lett.*, *120*, 055102.

Halekas, J. S. (2017, May). Seasonal variability of the hydrogen exosphere of mars. *Journal of Geophysical Research: Planets*, *122*(5), 901–911. Retrieved from https://doi.org/10.1002/2017je005306 doi: 10.1002/2017je005306

Halekas, J. S., Ruhunusiri, S., Harada, Y., Collinson, G., Mitchell, D. L., Mazelle, C., ... Jakosky, B. M. (2017, January). Structure, dynamics, and seasonal variability of the mars-solar wind interaction: MAVEN solar wind ion analyzer in-flight performance and science results. *Journal of Geophysical Research: Space Physics*, *122*(1), 547–578. Retrieved from https://doi.org/10.1002/2016ja023167 doi: 10.1002/2016ja023167

Halekas, J. S., Taylor, E., Dalton, G., Johnson, G., Curtis, D., McFadden, J., ... Jakosky, B. (2015). The solar wind ion analyzer for maven. *Space Science Reviews*, *195*(1-4), 125–151.

Hellinger, P., Verdini, A., Landi, S., Franci, L., & Matteini, L. (2018). von kármán–howarth equation for hall magnetohydrodynamics: Hybrid simulations. *The Astrophysical Journal Letters*, *857*(2), L19.

Hendrix, D., & Van Hoven, G. (1996). Magnetohydrodynamic turbulence and implications for solar coronal heating. *The Astrophysical Journal*, *467*, 887.

Jakosky, B. M., Grebowsky, J. M., Luhmann, J. G., Connerney, J., Eparvier, F., Ergun, R., ... others (2015b). Maven observations of the response of mars to an interplanetary coronal mass ejection. *Science*, *350*(6261), aad0210.

Jakosky, B. M., Lin, R., Grebowsky, J., Luhmann, J., Mitchell, D., Beutelschies, G., ... others (2015a). The mars atmosphere and volatile evolution (maven) mission. *Space Science Reviews*, *195*(1-4), 3-48.

Kolmogorov, A. N. (1941a). Dissipation of energy in locally isotropic turbulence. In *Dokl. akad. nauk sssr* (Vol. 32, pp. 16–18).

Kolmogorov, A. N. (1941b). The local structure of turbulence in incompressible viscous fluid for very large reynolds numbers. In *Dokl. akad. nauk sssr* (Vol. 30, pp. 299–303).

Leamon, R. J., Matthaeus, W. H., Smith, C. W., & Wong, H. K. (1998). Contribution of cyclotron-resonant damping to kinetic dissipation of interplanetary turbulence. *The Astrophysical Journal Letters*, *507*(2), L181.

Liu, D., Yao, Z., Wei, Y., Rong, Z., Shan, L., Arnaud, S., ... Wan, W. (2020). Upstream proton cyclotron waves: occurrence and amplitude dependence on IMF cone angle at mars — from MAVEN observations. *Earth and Planetary Physics*, *4*(1), 1–11. Retrieved from https://doi.org/10.26464/epp2020002 doi: 10.26464/epp2020002

Ma, Y., Fang, X., Russell, C. T., Nagy, A. F., Toth, G., Luhmann, J. G., ... Dong, C. (2014, October). Effects of crustal field rotation on the solar wind plasma interaction with mars. *Geophysical Research Letters*, *41*(19), 6563–6569. Retrieved from https://doi.org/10.1002/2014gl060785 doi: 10.1002/2014gl060785

MacBride, B. T., Smith, C. W., & Forman, M. A. (2008). *Astrophys. J.*, *679*, 1644-1660.

Marino, R., Sorriso-Valvo, L., Carbone, V., Noullez, A., Bruno, R., & Bavassano, B. (2008). Heating the Solar Wind by a Magnetohydrodynamic Turbulent Energy Cascade. *Astrophys. J. Lett.*, *677*.

Marquette, M. L., Lillis, R. J., Halekas, J., Luhmann, J., Gruesbeck, J., & Espley, J. (2018). Autocorrelation study of solar wind plasma and imf properties as measured by the maven spacecraft. *Journal of Geophysical Research: Space Physics*, *123*(4), 2493–2512.

Matthaeus, W., & Velli, M. (2011). Who needs turbulence? *Space science reviews*, *160*(1-4), 145.

Matthaeus, W. H., & Goldstein, M. (1982). Measurement of the rugged invariants of magnetohydrodynamic turbulence in the solar wind. *J. Geophys. Res.*, *87*(A8), 6011-6028.

Matthaeus, W. H., Zank, G. P., Smith, C. W., & Oughton, S. (1999). *Phys. Rev. Lett.*, *82*, 3444-.

Mazelle, C., & Neubauer, F. M. (1993). Discrete wave packets at the proton cyclotron frequency at comet p/halley. *Geophysical research letters*, *20*(2), 153–156.

Mazelle, C., Winterhalter, D., Sauer, K., Trotignon, J., Acuna, M., Baumgärtel, K., ... others (2004). Bow shock and upstream phenomena at mars. In *Mars' magnetism and its interaction with the solar wind* (pp. 115–181). Springer.

Modolo, R., Chanteur, G. M., & Dubinin, E. (2012, January). Dynamic martian magnetosphere: Transient twist induced by a rotation of the IMF. *Geophysical Research Letters*, *39*(1), n/a–n/a. Retrieved from https://doi.org/10.1029/2011gl049895 doi: 10.1029/2011gl049895

Osman, K. T., Matthaeus, W. H., Kiyani, K. H., Hnat, B., & Chapman, S. C. (2013, Nov). Proton kinetic effects and turbulent energy cascade rate in the solar wind. *Phys. Rev. Lett.*, *111*, 201101. Retrieved from https://link.aps.org/doi/10.1103/PhysRevLett.111.201101 doi: 10.1103/PhysRevLett.111.201101

Politano, H., & Pouquet, A. (1998a). Dynamical length scales for turbulent magnetized flows. *Geophysical Research Letters*, *25*(3), 273–276.

Politano, H., & Pouquet, A. (1998b). von kármán–howarth equation for magnetohydrodynamics and its consequences on third-order longitudinal structure and correlation functions. *Physical Review E*, *57*(1), R21.

Rahmati, A., Larson, D. E., Cravens, T. E., Lillis, R. J., Halekas, J. S., McFadden, J. P., ... Jakosky, B. M. (2017, March). MAVEN measured oxygen and hydrogen pickup ions: Probing the martian exosphere and neutral escape. *Journal of Geophysical Research: Space Physics*, *122*(3), 3689–3706. Retrieved from https://doi.org/10.1002/2016ja023371 doi: 10.1002/2016ja023371

Roberts, D., Goldstein, M., & Klein, L. (1990). The amplitudes of interplanetary fluctuations: Stream structure, heliocentric distance, and frequency dependence. *Journal of Geophysical Research: Space Physics*, *95*(A4), 4203–4216.

Romanelli, N., Bertucci, C., Gomez, D., Mazelle, C., & Delva, M. (2013). Proton cyclotron waves upstream from mars: Observations from mars global surveyor. *Planetary and Space Science*, *76*, 1–9.

Romanelli, N., DiBraccio, G., Modolo, R., Leblanc, F., Espley, J., Gruesbeck, J., ... Jakosky, B. (2019, October). Recovery timescales of the dayside martian magnetosphere to IMF variability. *Geophysical Research Letters*, *46*(20), 10977–10986. Retrieved from https://doi.org/10.1029/2019gl084151 doi: 10.1029/2019gl084151

Romanelli, N., Mazelle, C., Chaufray, J.-Y., Meziane, K., Shan, L., Ruhunusiri, S., ... others (2016). Proton cyclotron waves occurrence rate upstream from mars observed by maven: Associated variability of the martian upper atmosphere. *Journal of Geophysical Research: Space Physics*, *121*(11), 11–113.

Romanelli, N., Modolo, R., Leblanc, F., Chaufray, J.-Y., Hess, S., Brain, D., ... Jakosky, B. (2018b). Effects of the crustal magnetic fields and changes in the imf orientation on the magnetosphere of mars: Maven observations and lathys results. *Journal of Geophysical Research: Space Physics*, *123*(7), 5315–5333.

Romanelli, N., Modolo, R., Leblanc, F., Chaufray, J. Y., Martinez, A., Ma, Y., ... Holmström, M. (2018a, August). Responses of the martian magnetosphere to an interplanetary coronal mass ejection: MAVEN observations and LatHyS results. *Geophysical Research Letters*, *45*(16), 7891–7900. Retrieved from https://doi.org/10.1029/2018gl077714 doi: 10.1029/2018gl077714

Ruhunusiri, S., Halekas, J., Espley, J., Mazelle, C., Brain, D., Harada, Y., ... others (2017). Characterization of turbulence in the mars plasma environment with maven observations. *Journal of Geophysical Research: Space Physics*, *122*(1), 656–674.

Ruhunusiri, S., Halekas, J. S., Connerney, J. E. P., Espley, J. R., McFadden, J. P., Larson, D. E., ... Jakosky, B. M. (2015, November). Low-frequency waves in the martian magnetosphere and their response to upstream solar wind driving conditions. *Geophysical Research Letters*, *42*(21), 8917–8924. Retrieved from https://doi.org/10.1002/2015gl064968 doi: 10.1002/2015gl064968

Ruhunusiri, S., Halekas, J. S., Connerney, J. E. P., Espley, J. R., McFadden, J. P., Mazelle, C., ... Jakosky, B. M. (2016, March). MAVEN observation of an obliquely propagating low-frequency wave upstream of mars. *Journal of Geophysical Research: Space Physics*, *121*(3), 2374–2389. Retrieved from https://doi.org/10.1002/2015ja022306 doi: 10.1002/2015ja022306

Russell, C., Luhmann, J., Schwingenschuh, K., Riedler, W., & Yeroshenko, Y. (1990). Upstream waves at mars: Phobos observations. *Geophysical Research Letters*, *17*(6), 897–900.

Sahraoui, F., Goldstein, M., Robert, P., & Khotyaintsev, Y. V. (2009). Evidence of a cascade and dissipation of solar-wind turbulence at the electron gyroscale. *Physical review letters*, *102*(23), 231102.

Sahraoui, F., Hadid, L., & Huang, S. (2020). Magnetohydrodynamic and kinetic scale turbulence in the near-earth space plasmas: a (short) biased review. *Reviews of Modern Plasma Physics*, *4*(1), 1–33.

Sorriso-Valvo, L., Marino, R., Carbone, V., Noullez, A., Lepreti, F., Veltri, P., ... Pietropaolo, E. (2007). Observation of inertial energy cascade in interplanetary space plasma. *Physical review letters*, *99*(11), 115001.

Weygand, J. M., Matthaeus, W. H., Dasso, S., Kivelson, M. G., & Walker, R. J. (2007). Taylor scale and effective magnetic reynolds number determination from plasma sheet and solar wind magnetic field fluctuations. *J. Geophys. Res.: Space Phys.*, *112*, A10.

Wu, C., & Hartle, R. (1974). Further remarks on plasma instabilities produced by ions born in the solar wind. *Journal of Geophysical Research*, *79*(1), 283–285.

Wu, C. S., & Davidson, R. C. (1972, October). Electromagnetic instabilities produced by neutral-particle ionization in interplanetary space. *Journal of Geophysical Research*, *77*(28), 5399–5406. Retrieved from https://doi.org/10.1029/ja077i028p05399 doi: 10.1029/ja077i028p05399

Yamauchi, M., Hara, T., Lundin, R., Dubinin, E., Fedorov, A., Sauvaud, J.-A., ... Barabash, S. (2015, December). Seasonal variation of martian pick-up ions: Evidence of breathing exosphere. *Planetary and Space Science*, *119*, 54–61. Retrieved from https://doi.org/10.1016/j.pss.2015.09.013 doi: 10.1016/j.pss.2015.09.013
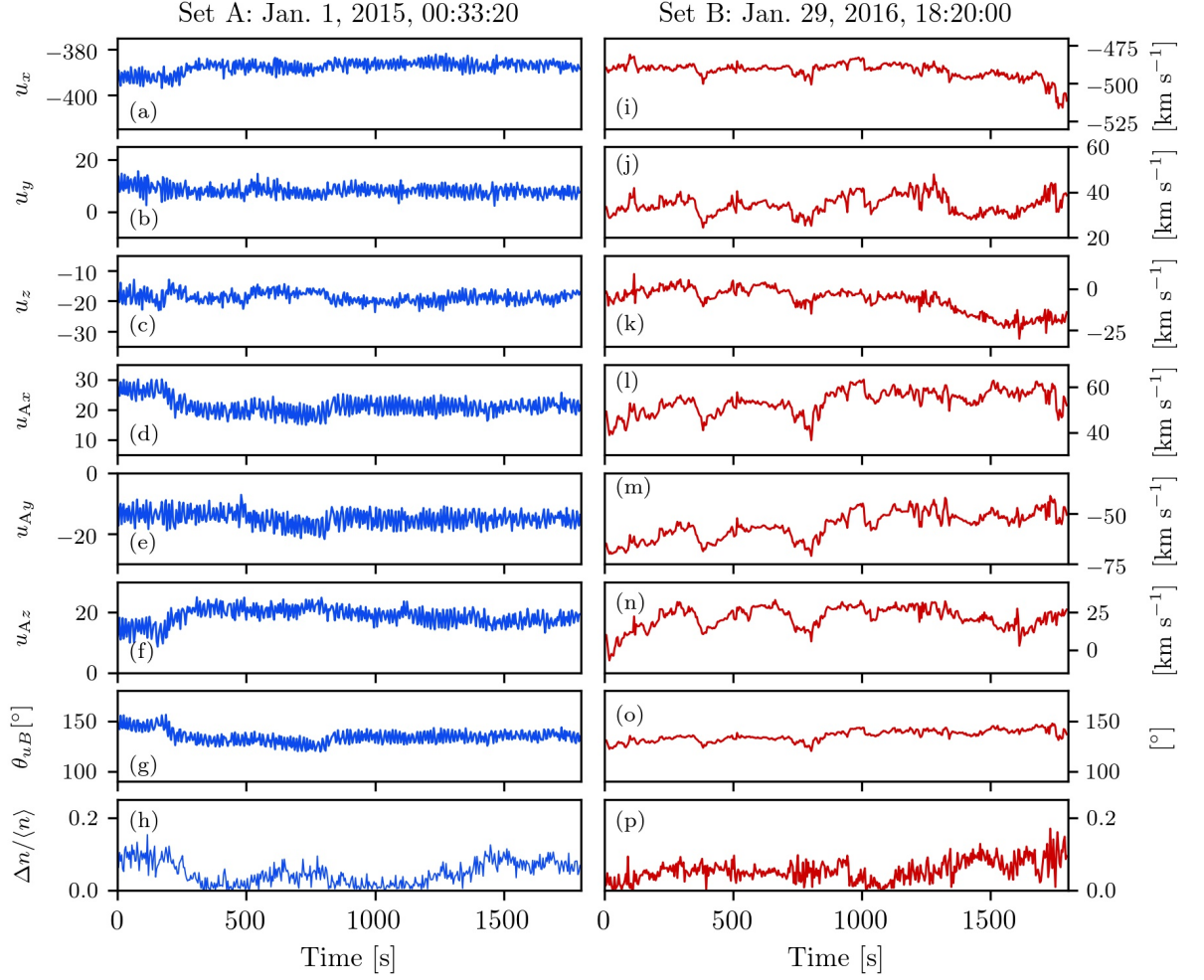
Figure 1. Time series for two examples from sets A and B. In particular, the proton and Alfvén velocity field components (in MSO coordinate system), the angle between magnetic and velocity fields and the density fluctuation level, respectively.
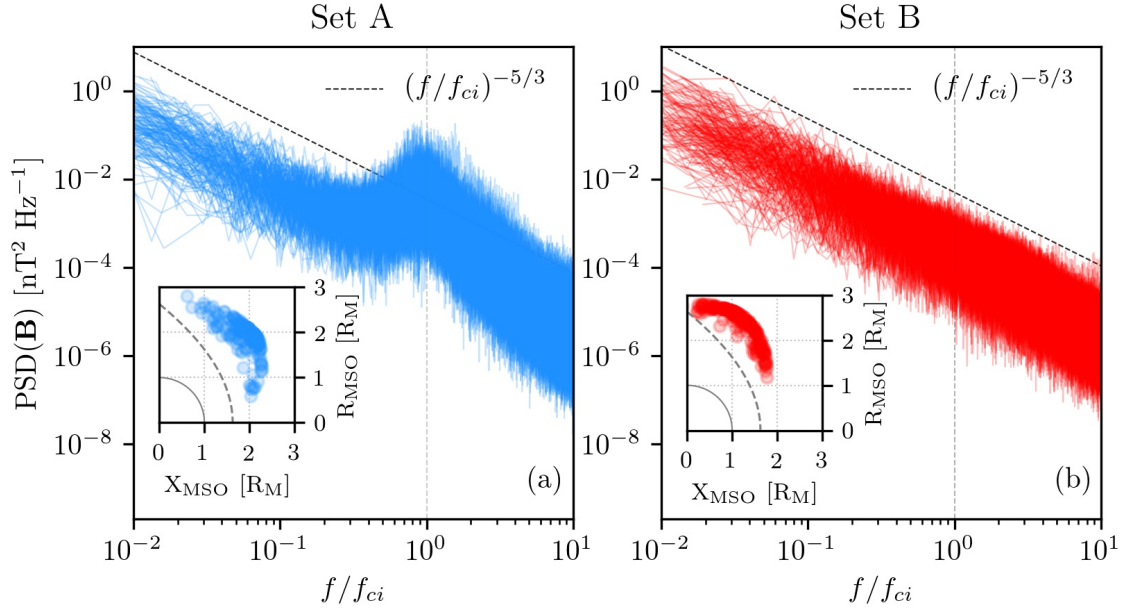
Figure 2. Magnetic power spectra density for both sets A and B, respectively. Inset: MAVEN location of each event in MSO reference frame and the bow shock best fit.
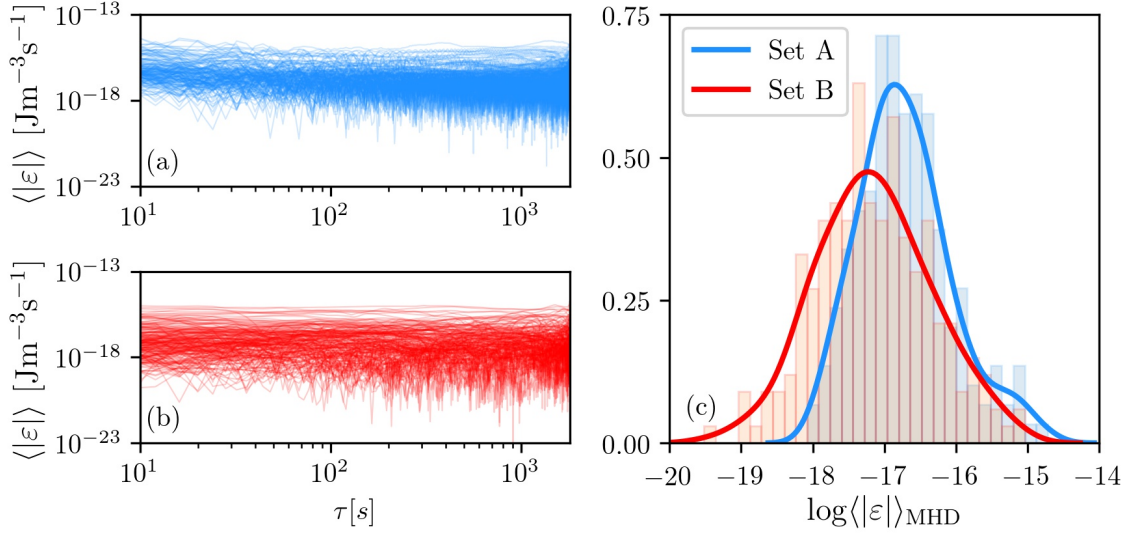
Figure 3. Energy cascade rate (absolute value) as a function of the time lag for sets (a) A and (b) B, respectively. (c) Histogram of $\log\langle|\varepsilon|\rangle_{\mathrm{MHD}}$ for both sets.
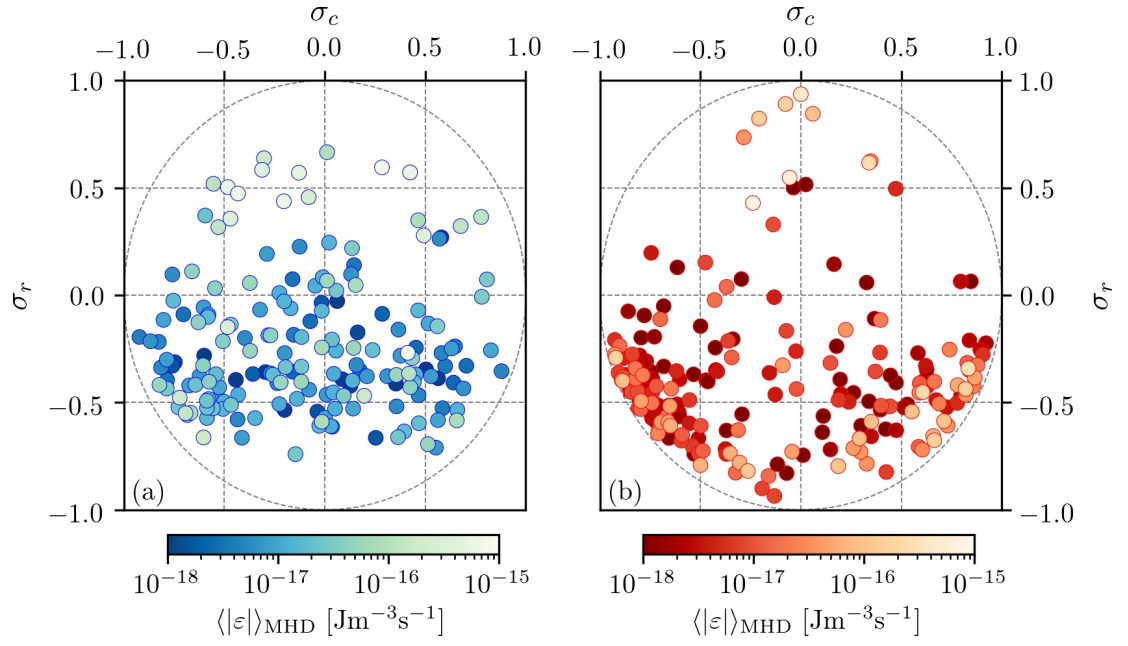
Figure 4. Scatter plot of σ_r as a function of σ_r for both sets A and B, respectively. Color bars correspond to the mean cascade rate in the MHD scales.